Hybrid Beamforming Design for OFDM Dual-Function Radar-Communication System with Double-Phase-Shifter Structure

Bowen Wang[1], Ziyang Cheng[1,2], Linlong Wu[3] and Zishu He[1]
[1]Sch. of Information & Communication Eng., University of Electronic Science and Technology of China
[2]Guangdong Key Lab. of Intelligent Information Processing & Shenzhen Key Lab. of Media Security
[3]Interdisciplinary Centre for Security, Reliability and Trust (SnT), University of Luxembourg

***Abstract*—In this paper, the problem of the hybrid beamforming (HBF) for a millimeter wave (mmWave) orthogonal frequency division multiplexing (OFDM) dual-function radar-communication (DFRC) system in the presence of signal-dependent interference is studied. The HBF network is based on the subarray connection architecture combining with the double-phase-shifter (DPS) structure. To achieve the dual functionality, we formulate the problem by maximizing the communication spectral efficiency subject to the constraints of radar integrated side-lobe to main-lobe ratio (ISMR), space-frequency nulling (SFN) and energy. An efficient algorithm based on the consensus alternating direction method of multipliers (CADMM) framework is developed to tackle the resultant nonconvex problem. Simulation results demonstrate the superiority of the proposed DPS structure and HBF algorithm.**

***Index Terms*—Hybrid beamforming (HBF), mmWave, OFDM-DFRC, double-phase-shifter (DPS).**

I. Introduction

Due to the enormous demand for wireless data services and internet of things (IoT) applications, wireless communication and intelligent sensing systems are now ubiquitously deployed. Under this background, in many emerging applications, sensing and communication are envisioned as a pair of intertwined functionalities [1]. In light of the above, the dual-function radar-communication (DFRC) system, where radar and communication share a common platform, has been regarded as a more favorable approach [2]–[9].

With mmWave communications emerging as the preferred technology for 5G and beyond 5G (B5G), many researchers devote themselves to the design of mmWave DFRC systems equipped with hybrid beamforming (HBF) structure [10]–[13] which is a promising technology for mmWave. For instance, the work of [10] proposes a novel framework for the DFRC base station (BS) equipped with a fully-connected HBF structure. Although this method can provide satisfactory performance for both radar and communication sides, it causes a large power budget due to tremendous phase shifters (PSs). To cope with this issue, the authors in [12] propose using the sub-connected structure to implement a DFRC system, where the communication rate is maximized under radar pattern similarity and energy constraints. Since the sub-connected structure employs much fewer PS, it causes non-negligible degradation of the degree of freedom (DoF), making it difficult for such structures to achieve satisfactory performance.

As mentioned above, there is no comprehensive HBF structure to efficiently achieve a satisfactory trade-off between performance and hardware cost, which motivates us to carry out this study to find a more favorable structure. Towards this end, we propose a novel OFDM-DFRC system equipped with DPS based HBF structure, which achieves the above desired trade-off in the sense of boosting the performance with only a moderate increase of required PSs. Although similar DPS implementation in the HBF communication system was considered in [17]–[19], the DFRC system equipped with this new implementation has not been exploited, which will be illustrated in this paper.

Moreover, in the existing literature on the OFDM-DFRC systems, mutual information [8], detection probability [9] and beampattern similarity property [13] are usually selected as radar metrics. Such metric, however, would lead to high side-lobe range, which challenges the practical application of this approach. To the best of our knowledge, the design of an OFDM-DFRC waveform with rigorous side-lobe control has not been studied. Moreover, the existing works on the OFDM-DFRC systems do not consider the signal-dependent interferences, further limiting their applicability in practical DFRC scenarios.

Motivated by the above, in this paper, we introduce a novel metric, i.e., integrated side-lobe to main-lobe ratio (ISMR), to control side-lobe energy effectively. Additionally, a robust space-frequency nulling (SFN) is enforced to suppress the strong unwanted return coursed by interferences. In terms of the corresponding HBF design, the hybrid beamformers are optimized to maximize the communication spectral efficiency under the radar ISMR, SFN, DPS and power constraints. To efficiently solve this non-convex problem, we propose an alternating optimization method under the CADMM [14] framework. Simulation results demonstrate the effectiveness of the proposed novel DPS structure and corresponding design algorithm.

Notation: $(\cdot)^T$ and $(\cdot)^H$ represent the transpose and conjugate transpose operators, respectively. $\mathrm{tr}(\mathbf{A})$ denotes the trace of $\mathbf{A}$. The operator $\mathbf{A}\left[i,j\right]$ the (i,j)-th element of the matrix $\mathbf{A}$. $|\cdot|$ represents determinant or absolute value depending on context. $\|\cdot\|_F$ denotes the Frobenius norm, and $\mathrm{Bdiag}(\cdot)$ denotes block diagonal matrix.

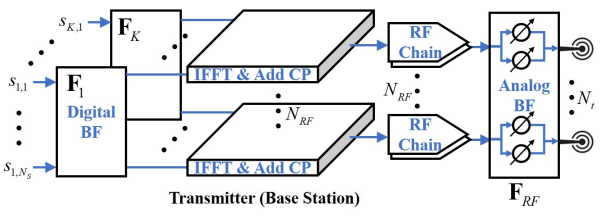

Fig. 1. Overview of the wideband OFDM-DFRC system equipped with DPS based hybrid beamforming structure.

II. Problem Formulation

As depicted in Fig. 1, we consider a mmWave wideband OFDM-DFRC system equipped with DPS based sub-connected HBF structure. The DFRC system with K subcarriers employs a uniform linear array (ULA) with N_t antennas and N_{RF} RF chains to send N_s data symbols per frequency subcarrier to N_u downlink users, which are equipped with fully digital structure with M_r antennas. Meanwhile, the DFRC system transmits radar waveforms to detect the targets of interest in the presence of multiple strong interferences.

A. Transmit Model

The transmit signal $\mathbf{x}_k \in \mathbb{C}^{N_t}$ at k-th subcarrier can be expressed as

$$\mathbf{x}_k = \mathbf{F}_{RF}\mathbf{F}_k\mathbf{s}_k = \mathbf{F}_{RF}\sum_{u=1}^{N_u}\mathbf{f}_{u,k}s_{u,k}, \tag{1}$$

where $s_{u,k}$ is the data symbol at k-th subcarrier for user u, $\mathbf{s}_k = [s_{1,k}, \cdots, s_{N_u,k}]^T$ denotes the vector of transmitted data symbols at k-th subcarrier with $\mathbb{E}\left(\mathbf{s}_k\mathbf{s}_k^H\right) = \mathbf{I}_{N_s}, \forall k$, $\mathbf{F}_{RF} \in \mathbb{C}^{N_t \times N_{RF}}$ and $\mathbf{F}_k = [\mathbf{f}_{1,k}, \cdots, \mathbf{f}_{N_u,k}] \in \mathbb{C}^{N_{RF} \times N_u}, \forall k$ stand for analog and digital beamformer, respectively. In this paper, we consider a novel sub-connected structure in which DPS in a parallel manner are equipped for the RF chains. Mathematically, $\mathbf{F}_{RF}$ can be expressed as

$$\mathbf{F}_{RF} = \mathrm{Bdiag}\left(\mathbf{p}_1, \mathbf{p}_2, \cdots, \mathbf{p}_{N_{RF}}\right) \tag{2}$$

where $\mathbf{p}_i \in \mathbb{C}^{N_t/N_{RF}}, \forall i$ with $\mathbf{p}_i[j] = e^{\jmath\varphi_{i,j}^1} + e^{\jmath\varphi_{i,j}^2} = A_{i,j}e^{\jmath\varphi_{i,j}}, \forall i,j$, and $A_{i,j} \in [0,2], \varphi_{i,j} \in [0, 2\pi)$. By this consideration, the constraint of $\mathbf{F}_{RF}$ is given by $\mathcal{F}_{RF} = \{\mathbf{F}_{RF} = \mathrm{Bdiag}\left(\mathbf{p}_1, \cdots, \mathbf{p}_{N_{RF}}\right), \mathbf{p}_i[j] = A_{i,j}e^{\jmath\varphi_{i,j}}, \forall i,j\}$.

B. Communication Model

After processing by a digital beamformer $\mathbf{w}_{u,k} \in \mathbb{C}^{M_r}$, the received signal at k-th subcarrier for u-th user is given by

$$\begin{aligned}\hat{s}_{u,k} =& \mathbf{w}_{u,k}^H\mathbf{H}_{u,k}\mathbf{F}_{RF}\mathbf{f}_{u,k}s_{u,k} + \mathbf{w}_{u,k}^H\mathbf{H}_{u,k}\mathbf{F}_{RF}\sum_{\ell\neq u}^{N_u}\mathbf{f}_{\ell,k}s_{\ell,k} \\ &+ \mathbf{w}_{u,k}^H\mathbf{n}_{u,k},\end{aligned} \tag{3}$$

where $\mathbf{n}_{u,k} \sim \mathcal{CN}\left(0, \sigma_n^2\mathbf{I}_{M_r}\right), \forall u,k$ is independently and identically distributed complex Gaussian noise, and $\mathbf{H}_{u,k} \in \mathbb{C}^{M_r \times N_t}, \forall u,k$ stands for the channel for u-th user at the k-th subcarrier. Thus, the spectral efficiency for user u at k-th sub-carrier can be written as

$$\mathrm{R}_{u,k} = \log\left(1 + \frac{\left|\mathbf{w}_{u,k}^H\mathbf{H}_{u,k}\mathbf{F}_{RF}\mathbf{f}_{u,k}\right|^2}{\sum\limits_{\ell\neq u}\left|\mathbf{w}_{u,k}^H\mathbf{H}_{u,k}\mathbf{F}_{RF}\mathbf{f}_{\ell,k}\right|^2 + \sigma_n^2\mathbf{w}_{u,k}^H\mathbf{w}_{u,k}}\right). \tag{4}$$

C. Radar Model

For wideband radar function, to effectively control side-lobe energy, we propose to minimize the beampattern integrated side-lobe to main-lobe ratio (ISMR), which is defined as

$$\begin{aligned}\mathrm{ISMR}(k) &= \frac{\int_{\Delta t}\int_{\Theta_s}\left|\mathbf{a}^H(f_k,\theta)\mathbf{x}(t)\right|^2\mathrm{d}\theta\mathrm{d}t}{\int_{\Delta t}\int_{\Theta_m}\left|\mathbf{a}^H(f_k,\theta)\mathbf{x}(t)\right|^2\mathrm{d}\theta\mathrm{d}t} \\ &= \frac{\mathrm{tr}\left\{\mathbf{F}_{RF}\mathbf{F}_k\mathbf{F}_k^H\mathbf{F}_{RF}^H\mathbf{\Omega}_{s,k}\right\}}{\mathrm{tr}\left\{\mathbf{F}_{RF}\mathbf{F}_k\mathbf{F}_k^H\mathbf{F}_{RF}^H\mathbf{\Omega}_{m,k}\right\}},\end{aligned} \tag{5}$$

where $\mathbf{\Omega}_{s,k} = \int_{\Theta_s}\mathbf{a}(f_k,\theta)\mathbf{a}^H(f_k,\theta)\mathrm{d}\theta$ and $\mathbf{\Omega}_{m,k} = \int_{\Theta_m}\mathbf{a}(f_k,\theta)\mathbf{a}^H(f_k,\theta)\mathrm{d}\theta$ with Θ_s and Θ_m being side-lobe and main-lobe region, respectively. $\mathbf{a}(f,\theta)$ denotes the space-frequency steering vector of transmit array, which is defined as $\mathbf{a}(f,\theta) = \left[1, e^{2\pi f\frac{\delta\sin\theta}{c}}, \cdots, e^{2\pi f\frac{(N_t-1)\delta\sin\theta}{c}}\right]^T$.

To effectively avoid the unwanted return from strong interference, we enforce the space-frequency nulling (SFN) at the interference's direction, which is defined as

$$\mathrm{SFN}(k) = \sum_{i=1}^{I_k}\int_{\Delta t}\left|\mathbf{a}(f_k,\vartheta_{k,i})\mathbf{x}(t)\right|\mathrm{d}t \leqslant I_k\Gamma_k \tag{6}$$

where Γ_k denotes the maximum power that can be radiated towards the interference's directions included in the set $\vartheta_k = [\vartheta_{k,1}, \vartheta_{k,2}, \cdots, \vartheta_{k,I_k}]$.

Note that constraint (6) can only achieve sharp nulls in transmit waveform so that the fast-moving interference may escape from the nulls. To this end, the robust SFN constraint is defined as

$$\begin{aligned}\overline{\mathrm{SFN}}(k) &= \sum_{i=1}^{I_k}\int_{\Delta t}\int_{\Theta_{N_{k,i}}}\left|\mathbf{a}(f_k,\theta)\mathbf{x}(t)\right|\mathrm{d}\theta\mathrm{d}t \\ &= \mathrm{tr}\left\{\mathbf{F}_{RF}\mathbf{F}_k\mathbf{F}_k^H\mathbf{F}_{RF}^H\mathbf{A}_k\right\} \leqslant \overline{\Gamma}_k\end{aligned} \tag{7}$$

where $\mathbf{A}_k = \sum_{i=1}^{I_k}\int_{\Theta_{N_{k,i}}}\mathbf{a}(f_k,\theta)\mathbf{a}^H(f_k,\theta)\mathrm{d}\theta$ and $\Theta_{N_{k,i}} = \left[\vartheta_{N_{k,i}} - \frac{\delta}{2}, \vartheta_{N_{k,i}} + \frac{\delta}{2}\right]$ with δ being the angle uncertainty.

D. Problem Formulation

According to the above system model, our problem of interest can be formulated as

$$\max_{\substack{\mathbf{F}_{RF},\{\mathbf{F}_k\},\\ \{\mathbf{w}_{u,k}\}}} \frac{1}{K}\sum_{k=1}^{K}\sum_{u=1}^{N_u}\mathrm{R}_{u,k} \tag{8a}$$

$$\text{s.t.} \quad \mathrm{ISMR}(k) \leqslant \gamma_k, \forall k \tag{8b}$$

$$\overline{\mathrm{SFN}}(k) \leqslant \overline{\Gamma}_k, \forall k \tag{8c}$$

$$\|\mathbf{F}_{RF}\mathbf{F}_k\|_F^2 = \mathrm{P}_k, \forall k \tag{8d}$$

$$\mathbf{F}_{RF} \in \mathcal{F}_{RF}, \tag{8e}$$

where the constraint (8b) is the ISMR requirement for the radar, γ_k is threshold of ISMR at k-th subcarrier, the constraint (8c) denotes the space-frequency nulling condition, the constraint (8d) is the energy budget, and the constraint (8e) stands for the DPS constraint of transmitting analog beamformer. Note that due to the complicated objective (8a) and the nonconvex inequality constraint (8b), the problem (8) is NP-hard and generally challenging to solve.

Before we tackle the problem (8) directly, we first reformulate it into a more tractable form based on the WMMSE technique [15] as follows:

$$\min_{\mathbf{F}_{RF},\{\mathbf{F}_k\},\{\mathbf{w}_{u,k}\}} \frac{1}{K}\sum_{u=1}^{N_u} \mathrm{tr}\left\{\aleph_{u,k}^t \mathcal{E}_{u,k}\left(\mathbf{F}_{RF},\mathbf{F}_k,\mathbf{w}_{u,k}\right)\right\} \quad (9)$$
$$\text{s.t.} \qquad (8b)-(8e),$$

where $\aleph_{u,k}^t = \mathcal{E}_{u,k}^{-1}\left(\mathbf{T}_k^t,\mathbf{w}_{u,k}^t\right)$ and $\mathcal{E}_{u,k}\left(\mathbf{F}_{RF},\mathbf{F}_k,\mathbf{w}_{u,k}\right)$ is defined as

$$\mathcal{E}_{u,k}\left(\mathbf{F}_{RF},\mathbf{F}_k,\mathbf{w}_{u,k}\right) = \mathbb{E}\left[\left(\hat{s}_{u,k}-s_{u,k}\right)\left(\hat{s}_{u,k}-s_{u,k}\right)^H\right]$$
$$= \left|\mathbf{w}_{u,k}^H\mathbf{H}_{u,k}\mathbf{F}_{RF}\mathbf{f}_{u,k}-1\right|^2 + \sum_{\ell\neq u}^{N_u}\left|\mathbf{w}_{u,k}^H\mathbf{H}_{u,k}\mathbf{F}_{RF}\mathbf{f}_{\ell,k}\right|^2 + \sigma_n^2\mathbf{w}_{u,k}^H\mathbf{w}_{u,k}.$$

After the above transformation, problem (9) is still a high-dimension and non-convex optimization problem. In the following, we will solve this challenging problem with the aid of alternating optimization procedure [14].

III. Solution to Optimization Problem (7)

To facilitate the CADMM framework development, we first introduce auxiliary variables $\{\mathbf{T}_k\}$,$\{\mathbf{V}_k\}$ and $\{\mathbf{Y}_k\}$ to decouple the variables $\mathbf{F}_{RF}$ and $\{\mathbf{F}_k\}$. Thus, the problem (9) can be rewritten as,

$$\min_{\substack{\mathbf{F}_{RF},\{\mathbf{F}_k\},\{\mathbf{w}_{u,k}\}\\ \{\mathbf{T}_k\},\{\mathbf{V}_k\},\{\mathbf{Y}_k\}}} \frac{1}{K}\sum_{u=1}^{N_u} \mathrm{tr}\left\{\aleph_{u,k}^t \mathcal{E}_{u,k}\left(\mathbf{T}_k,\mathbf{w}_{u,k}\right)\right\} \quad (10a)$$
$$\text{s.t.} \quad \mathbf{T}_k = \mathbf{V}_k = \mathbf{Y}_k = \mathbf{F}_{RF}\mathbf{F}_k, \forall k \quad (10b)$$
$$\mathrm{tr}\left\{\mathbf{V}_k\mathbf{V}_k^H\mathbf{\Omega}_k\right\} \leqslant 0, \forall k \quad (10c)$$
$$\mathrm{tr}\left\{\mathbf{Y}_k\mathbf{Y}_k^H\mathbf{A}_k\right\} \leqslant \bar{\Gamma}_k, \forall k \quad (10d)$$
$$\left\|\mathbf{T}_k\right\|_F^2 = \mathrm{P}, \forall k \quad (10e)$$
$$\mathbf{F}_{RF} \in \mathcal{F}_{RF}, \quad (10f)$$

where $\mathbf{\Omega}_k = \mathbf{\Omega}_{s,k} - \gamma_k\mathbf{\Omega}_{m,k}$. Then, the optimal solution of the problem (10) can be obtained by minimizing its augmented Lagrangian function $\mathcal{L} = \sum_{k=1}^{K}\mathcal{L}_k\left(\mathbf{F}_{RF},\mathbf{F}_k,\mathbf{w}_{u,k},\mathbf{T}_k,\mathbf{V}_k,\mathbf{Y}_k\right)$, where $\mathcal{L}_k\left(\mathbf{F}_{RF},\mathbf{F}_k,\mathbf{w}_{u,k},\mathbf{T}_k,\mathbf{V}_k,\mathbf{Y}_k\right)$ is defined as

$$\mathcal{L}_k\left(\mathbf{F}_{RF},\mathbf{F}_k,\mathbf{w}_{u,k},\mathbf{T}_k,\mathbf{V}_k,\mathbf{Y}_k\right) = \frac{\rho_{1,k}}{2}\left\|\mathbf{T}_k-\mathbf{F}_{RF}\mathbf{F}_k+\frac{\mathbf{\Lambda}_{1,k}}{\rho_{1,k}}\right\|_F^2$$
$$+\frac{\rho_{2,k}}{2}\left\|\mathbf{T}_k-\mathbf{V}_k+\frac{\mathbf{\Lambda}_{2,k}}{\rho_{2,k}}\right\|_F^2 + \frac{\rho_{3,k}}{2}\left\|\mathbf{T}_k-\mathbf{Y}_k+\frac{\mathbf{\Lambda}_{3,k}}{\rho_{3,k}}\right\|_F^2$$
$$+\frac{1}{K}\sum_{u=1}^{N_u}\mathrm{tr}\left\{\aleph_{u,k}^t\mathcal{E}_{u,k}\left(\mathbf{T}_k,\mathbf{w}_{u,k}\right)\right\}$$

with $\mathbf{\Lambda}_{1,k},\mathbf{\Lambda}_{2,k},\mathbf{\Lambda}_{3,k} \in \mathbb{C}^{N_t\times N_s},\forall k$ and $\rho_{1,k},\rho_{2,k},\rho_{3,k} > 0$ being dual variables and corresponding penalty parameters, respectively. Under the CADMM framework, we update $\left(\{\mathbf{w}_{u,k}\},\{\mathbf{T}_k\},\{\mathbf{V}_k\},\{\mathbf{Y}_k\},\{\mathbf{F}_k\},\mathbf{F}_{RF}\right)$ via the following alternating iterative steps:

A. Optimization of $(\mathbf{w}_{u,k},\mathbf{T}_k,\mathbf{V}_k,\mathbf{Y}_k)$

With fixed $(\mathbf{F}_{RF},\mathbf{F}_k)$, $(\mathbf{w}_{u,k},\mathbf{T}_k,\mathbf{V}_k,\mathbf{Y}_k)$ are updated by solving the following problem

$$\min_{\mathbf{w}_{u,k},\mathbf{T}_k,\mathbf{V}_k,\mathbf{Y}_k} \mathcal{L}\left(\mathbf{w}_{u,k},\mathbf{T}_k,\mathbf{V}_k,\mathbf{Y}_k\right) \quad (11a)$$
$$\text{s.t.} \quad \mathrm{tr}\left\{\mathbf{V}_k\mathbf{V}_k^H\mathbf{\Omega}_k\right\} \leqslant 0 \quad (11b)$$
$$\mathrm{tr}\left\{\mathbf{Y}_k\mathbf{Y}_k^H\mathbf{A}_k\right\} \leqslant \bar{\Gamma}_k \quad (11c)$$
$$\left\|\mathbf{T}_k\right\|_F^2 = \mathrm{P}, \forall k. \quad (11d)$$

By leveraging the Karush-Kuhn-Tucker (KKT) conditions, the close-form solution to $\mathbf{T}_k$ can be calculated by

$$\mathbf{T}_k^\star\left(\mu_k\right) = \left\{\mathbf{\Phi}_k + 2\mu_k\mathbf{I}_{N_t}\right\}^{-1}\mathbf{\Upsilon}_k, \quad (12)$$

where the μ denotes the multiplier, $\mathbf{\Phi}_k$ and $\mathbf{\Upsilon}_k$ are defined as

$$\mathbf{\Phi}_k = \frac{2}{K}\sum_{u=1}^{N_u}\aleph_{u,k}^t\mathbf{H}_{u,k}^H\mathbf{w}_{u,k}\mathbf{w}_{u,k}^H\mathbf{H}_{u,k}\mathbf{T}_k + \left(\rho_{1,k}+\rho_{2,k}+\rho_{3,k}\right)\mathbf{I}_{N_t},$$
$$\mathbf{\Upsilon}_k = \frac{2}{K}\sum_{u=1}^{N_u}\aleph_{u,k}^t\mathbf{H}_{u,k}^H\mathbf{w}_{u,k}\mathbf{e}_u^H + \rho_{1,k}\mathbf{F}_{RF}\mathbf{F}_k + \rho_{2,k}\mathbf{T}_k + \rho_{3,k}\mathbf{Y}_k - \mathbf{\Lambda}_{1,k} - \mathbf{\Lambda}_{2,k} - \mathbf{\Lambda}_{3,k}.$$

Defining eigenvalue decomposition (EVD), i.e., $\mathbf{\Phi}_k = \mathbf{Q}_k\mathbf{D}_k\mathbf{Q}_k^H$, and substituting (12) into the power constraint (11d), one gets

$$\left\|\mathbf{T}_k^\star\left(\mu_k\right)\right\|_F^2 = \sum_{n=1}^{N_t}\frac{\left(\mathbf{Q}_k^H\mathbf{\Upsilon}_k\mathbf{\Upsilon}_k^H\mathbf{Q}_k\right)[n,n]}{\left(\mathbf{D}_k[n,n]+2\mu_k\right)^2} = \mathrm{P}. \quad (13)$$

Then, the optimal multiplier $\mu_k^\star$ can be easily obtained using the golden-section search or Newton's method [16]. Finally, plugging $\mu_k^\star$ into (12), we can obtain the solution to $\mathbf{T}_k$.

The solution to $\mathbf{V}_k$ can be obtained by the KKT condition. Specifically, via introducing multiplier $\chi_1 \geqslant 0$, the corresponding KKT conditions can be derived as

$$\mathbf{V}_k^\star = \left\{\rho_{2,k}\mathbf{I}_{N_t} + 2\chi_1\mathbf{\Omega}^H\right\}^{-1}\mathbf{\Psi}_k \quad (14a)$$
$$\chi_1\mathrm{tr}\left\{\mathbf{V}_k\mathbf{V}_k^H\mathbf{\Omega}_k\right\} = 0,\ \chi_1 \geqslant 0 \quad (14b)$$
$$\mathrm{tr}\left\{\mathbf{V}_k\mathbf{V}_k^H\mathbf{\Omega}_k\right\} \leqslant 0, \quad (14c)$$

where $\mathbf{\Psi}_k = \mathbf{\Lambda}_{2,k} + \rho_{2,k}\mathbf{T}_k$. According to KKT conditions (14), the optimal value of $\mathbf{V}_k$ satisfies the two cases:

Case 1: For $\chi_1 = 0$, from the (14a) we have $\mathbf{V}_k^\star = \mathbf{\Psi}_k/\rho_{2,k}$, which must satisfy the condition (14c), otherwise

Case 2: For $\chi_1 \neq 0$, from the (14a) we have

$$\mathbf{V}_k^\star\left(\chi_1\right) = \left\{\rho_{2,k}\mathbf{I}_{N_t} + 2\chi_1\mathbf{\Omega}^H\right\}^{-1}\mathbf{\Psi}_k, \quad (15)$$

which must satisfy $\mathrm{tr}\left\{\mathbf{V}_k\mathbf{V}_k^H\mathbf{\Omega}_k\right\} = 0$. Similar to previous approach to $\mathbf{T}_k$, after the EVD, i.e., $\mathbf{\Omega}_k^H = \mathbf{Z}_k\mathbf{M}_k\mathbf{Z}_k^H$ and

plugging (15) into $\mathrm{tr}\left\{\mathbf{V}_k\mathbf{V}_k^H\mathbf{\Omega}_k\right\}=0$, we obtain

$$\begin{aligned}&\mathrm{tr}\left\{\mathbf{V}_k^\star\left(\chi_1\right)\left(\mathbf{V}_k^\star\left(\chi_1\right)\right)^H\mathbf{\Omega}_k\right\}\\&=\sum_{n=1}^{N_t}\frac{\left(\mathbf{Z}_k^H\mathbf{\Omega}_k\mathbf{Z}_k\right)[n,n]\left(\mathbf{Z}_k^H\mathbf{\Psi}_k\mathbf{\Psi}_k^H\mathbf{Z}_k\right)[n,n]}{\left(\rho_{2,k}+2\chi_1\mathbf{M}_k[n,n]\right)^2}=0.\end{aligned}\tag{16}$$

It is obvious that the left-hand side (16) is strictly decreasing for $\chi_1>0$. Similar to the solution to (13), we can obtain the χ_1 via golden-section search.

Due to the similar form between $\mathbf{Y}_k$ and $\mathbf{V}_k$, we can update the $\mathbf{Y}_k$ via the same method. Hence, to avoid unnecessary duplication, we will omit the details of this procedure.

According to MMSE receiver, its optimal solution of $\mathbf{w}_{u,k}$ can be calculated as

$$\mathbf{w}_{u,k}=\left(\mathbf{H}_k\mathbf{T}_k\mathbf{T}_k^H\mathbf{H}_k^H-\mathbf{I}_{M_r}\right)^{-1}\mathbf{H}_k\mathbf{T}_k\left(:,n\right).\tag{17}$$

B. Optimization of $(\mathbf{F}_{RF},\mathbf{F}_k)$

With fixed $(\mathbf{w}_{u,k},\mathbf{T}_k,\mathbf{V}_k\ \ \mathbf{Y}_k)$ and $(\mathbf{\Lambda}_{1,k},\mathbf{\Lambda}_{2,k},\mathbf{\Lambda}_{3,k})$, $(\mathbf{F}_{RF},\mathbf{F}_k)$ are updated by solving the following problem

$$\begin{aligned}\min_{\mathbf{F}_{RF},\{\mathbf{F}_k\}}&\sum_{k=1}^{K}\frac{\rho_{1,k}}{2}\left\|\mathbf{T}_k-\mathbf{F}_{RF}\mathbf{F}_k+\frac{\mathbf{\Lambda}_{1,k}}{\rho_{1,k}}\right\|_F^2\\\text{s.t.}\quad&\mathbf{F}_{RF}\in\mathcal{F}_{RF}.\end{aligned}\tag{18}$$

The close-form solution of $\mathbf{F}_k$ is given by

$$\mathbf{F}_k=\left(\mathbf{F}_{RF}^H\mathbf{F}_{RF}\right)^{-1}\mathbf{F}_{RF}^H\left(\mathbf{T}_k+\frac{\mathbf{\Lambda}_{1,k}}{\rho_{1,k}}\right),\forall k.\tag{19}$$

Due to the block diagonal property of the analog beamformer, the corresponding problem of $\mathbf{F}_{RF}$ can be reformulated as

$$\min_{A_{i,j},\varphi_{i,j}}\sum_{k=1}^{K}\frac{\rho_{1,k}}{2}\left\|\widetilde{\mathbf{T}}_k[i,:]-A_{i,j}e^{\jmath\varphi_{i,j}}\mathbf{F}_k[j,:]\right\|_F^2,\forall i,\tag{20}$$

where $\widetilde{\mathbf{T}}_k=\mathbf{T}_k+\frac{\mathbf{\Lambda}_{1,k}}{\rho_{1,k}}$ and $j=\left\lceil i\frac{N_{RF}}{N_t}\right\rceil$. This is a basically vector approximation problem, whose close-form solution can be given by

$$A_{i,j}=\begin{cases}\frac{\sum_{k=1}^{K}\rho_{1,k}\left|\mathbf{F}_k[j,:]\mathbf{T}_k^H[i,:]\right|}{\sum_{k=1}^{K}\rho_{1,k}\|\mathbf{F}_k[j,:]\|_F^2}, & \frac{\sum_{k=1}^{K}\rho_{1,k}\left|\mathbf{F}_k[j,:]\mathbf{T}_k^H[i,:]\right|}{\sum_{k=1}^{K}\rho_{1,k}\|\mathbf{F}_k[j,:]\|_F^2}\leqslant 2\\2, & \text{otherwise},\end{cases}$$

and

$$\varphi_{i,j}=\mathrm{angle}\left(\sum_{k=1}^{K}\mathbf{F}_k[j,:]\,\mathbf{T}_k^H[i,:]\right).$$

After obtaining $A_{i,j}$ and $\varphi_{i,j}$, the close-form solution of $\varphi_{i,j}^1$ and $\varphi_{i,j}^2$ are calculated by

$$\begin{aligned}\varphi_{i,j}^1=&\varphi_{i,j}+\arccos\left(A_{i,j}/2\right),\\\varphi_{i,j}^2=&\varphi_{i,j}-\arccos\left(A_{i,j}/2\right).\end{aligned}\tag{21}$$

IV. Numerical Results

In all simulations, unless otherwise specified, we assume that the transmitter with $N_t=32$ antennas sends $N_s=4$ data streams per subcarrier to the receiver with $M_r=4$ antennas. The number of RF chains in the transmitter is $N_{RF}=8$. We assume that the number of subcarriers K is 128, the carrier frequency f_c is 10GHz and bandwidth B is 2.56GHz. For probing purpose, we assume the potential spatial sections of interest for the transmitter are main-lobe region $\Theta_m=[-10^\circ,10^\circ]$, thus, the side-lobe region $\Theta_s=[-90^\circ,-10^\circ)\cup(10^\circ,90^\circ]$. Furthermore, the space-frequency null azimuths ϑ_k are assumed as $\vartheta_k=\{-22^\circ,22^\circ\},\forall k$ with uncertainty $\delta=4^\circ$. The threshold Γ_k of the space-frequency nulls on k-th subcarrier is set as -40dB.

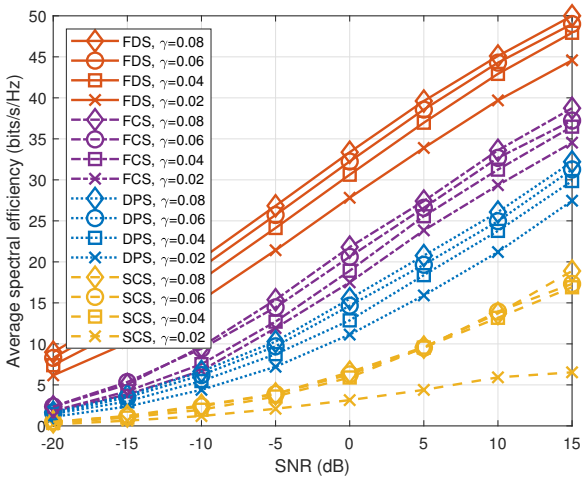

Fig. 2. Achievable SE versus SNR with different ISMR γ.

TABLE I
Comparison between different structures.

Structure	FCS	DPS	SCS
No. of PS	$N_tN_{RF}=256$	$2N_t=64$	$N_t=32$

In Fig. 2, we show the average spectral efficiency of the proposed algorithm versus SNR (SNR $=\mathrm{P}/\sigma_n^2$) for different ISMR γ. For comparison purposes, we also include the fully digital, sub-connected HBF and fully-connected HBF structures, which are denoted by "FDS", "SCS" and "FCS", respectively. Meanwhile, the corresponding numbers of the required PSs for "DPS", "SCS" and "FCS" are listed in Table I. From the results in Fig. 2, we observe that the attained spectral efficiency increases along with γ for all beamforming structures. As the value of γ increases, the radar constraint becomes less demanding to guarantee. In addition, we also find that the proposed DPS is able to significantly reduce the number of PSs than the FCS with a slight performance loss. While compared to the SPS, the DPS obtains a remarkable improvement in performance with only a moderate increase of PS. This means the proposed DPS achieves an excellent trade-off between the performance and hardware cost.

In Fig. 3, we compare the transmit space-frequency spectral behaviors of the designed hybrid transmit beamformers. It

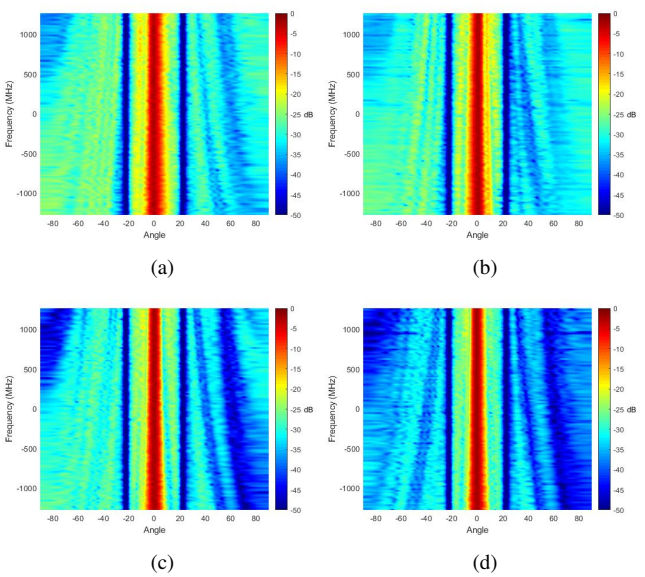

Fig. 3. The space-frequency spectral behaviors of the DPS based OFDM-DFRC with SNR=0dB and different ISMR value (1) γ = 0.08, (2) γ = 0.06, (3) γ = 0.04, (4) γ = 0.02.

can be observed that as the ISMR level γ decreases, the side-lobe energy becomes lower and lower, such that more energy is concentrated on the main-lobe. Therefore, we should choose a suitable γ to achieve a good trade-off between radar beampattern and communication spectral efficiency property. From the figure, we also note that the beampattern has desired space-frequency nulls at interference azimuth for all γ, which means energy value at interference azimuth is lower than the predefined threshold $\Gamma_k = -40$ dB. As expected, there exists the coupling effect between the angle and frequency, which is caused by the fixed analog beamformer $\mathbf{F}_{RF}$ for all subcarriers in the HBF structure.

V. Conclusion

In this paper, we have addressed the problem of the HBF design for the OFDM-DFRC system with the DPS structure. The corresponding problem is formulated to maximize the spectral efficiency subjecting to the power budget, SFN and the radar ISMR constraint. We propose an alternating optimization-based algorithm to tackle this non-convex problem. The simulation results show that the proposed method and novel structure can achieve satisfactory performance for radar and communication.

Acknowledgment

The work of Bowen Wang, Ziyang Cheng and Zishu He was supported by the National Natural Science Foundation of China (NSFC) (Grants NO.62001084 and NO.62031007), and the work of Linlong Wu was supported by FNR CORE SPRINGER under grant C18/IS/12734677.

References

[1] D. Ma, N. Shlezinger, T. Huang, Y. Liu and Y. C. Eldar, "Joint Radar-Communication Strategies for Autonomous Vehicles: Combining Two Key Automotive Technologies," in *IEEE Signal Processing Magazine*, vol. 37, no. 4, pp. 85-97, July 2020.

[2] F. Liu, L. Zhou, C. Masouros, A. Li, W. Luo and A. Petropulu, "Toward Dual-functional Radar-Communication Systems: Optimal Waveform Design," in *IEEE Transactions on Signal Processing*, vol. 66, no. 16, pp. 4264-4279, 15 Aug.15, 2018.

[3] F. Liu, C. Masouros, A. Li, H. Sun and L. Hanzo, "MU-MIMO Communications With MIMO Radar: From Co-Existence to Joint Transmission," in *IEEE Transactions on Wireless Communications*, vol. 17, no. 4, pp. 2755-2770, April 2018.

[4] Z. Cheng, S. Shi, Z. He and B. Liao, "Transmit Sequence Design for Dual-Function Radar-Communication System With One-Bit DACs," in *IEEE Transactions on Wireless Communications*, vol. 20, no. 9, pp. 5846-5860, Sept. 2021.

[5] M. L. Rahman, J. A. Zhang, X. Huang, Y. J. Guo and R. W. Heath, "Framework for a Perceptive Mobile Network Using Joint Communication and Radar Sensing," in *IEEE Transactions on Aerospace and Electronic Systems*, vol. 56, no. 3, pp. 1926-1941, June 2020.

[6] S. H. Dokhanchi, B. S. Mysore, K. V. Mishra and B. Ottersten, "A mmWave Automotive Joint Radar-Communications System," in *IEEE Transactions on Aerospace and Electronic Systems*, vol. 55, no. 3, pp. 1241-1260, June 2019.

[7] P. Kumari, J. Choi, N. González-Prelcic and R. W. Heath, "IEEE 802.11ad-Based Radar: An Approach to Joint Vehicular Communication-Radar System," in *IEEE Transactions on Vehicular Technology*, vol. 67, no. 4, pp. 3012-3027, April 2018.

[8] X. Yuan et al., "Spatio-Temporal Power Optimization for MIMO Joint Communication and Radio Sensing Systems With Training Overhead," in *IEEE Transactions on Vehicular Technology*, vol. 70, no. 1, pp. 514-528, Jan. 2021.

[9] T. Tian, T. Zhang, L. Kong and Y. Deng, "Transmit/Receive Beamforming for MIMO-OFDM Based Dual-Function Radar and Communication," in *IEEE Transactions on Vehicular Technology*, vol. 70, no. 5, pp. 4693-4708, May 2021, doi: 10.1109/TVT.2021.3072094.

[10] F. Liu, C. Masouros, A. P. Petropulu, H. Griffiths and L. Hanzo, "Joint Radar and Communication Design: Applications, State-of-the-Art, and the Road Ahead," in *IEEE Transactions on Communications*, vol. 68, no. 6, pp. 3834-3862, June 2020.

[11] F. Liu and C. Masouros, "Hybrid Beamforming with Sub-arrayed MIMO Radar: Enabling Joint Sensing and Communication at mmWave Band," *ICASSP 2019 - 2019 IEEE International Conference on Acoustics, Speech and Signal Processing (ICASSP)*, 2019, pp. 7770-7774.

[12] Z. Cheng, Z. He and B. Liao, "Hybrid Beamforming for Multi-Carrier Dual-Function Radar-Communication System," in *IEEE Transactions on Cognitive Communications and Networking*, vol. 7, no. 3, pp. 1002-1015, Sept. 2021.

[13] Z. Cheng, Z. He and B. Liao, "Hybrid Beamforming Design for OFDM Dual-Function Radar-Communication System," in *IEEE Journal of Selected Topics in Signal Processing*, vol. 15, no. 6, pp. 1455-1467, Nov. 2021.

[14] Boyd, Stephen, Neal Parikh, and Eric Chu, "Distributed optimization and statistical learning via the alternating direction method of multipliers," in *Now Publishers Inc*, 2011.

[15] Q. Shi, M. Razaviyayn, Z. Luo and C. He, "An Iteratively Weighted MMSE Approach to Distributed Sum-Utility Maximization for a MIMO Interfering Broadcast Channel," in *IEEE Transactions on Signal Processing*, vol. 59, no. 9, pp. 4331-4340, Sept. 2011.

[16] Conte, Samuel Daniel, and Carl De Boor. Elementary numerical analysis: an algorithmic approach. Society for Industrial and Applied Mathematics, 2017.

[17] T. E. Bogale, L. B. Le, A. Haghighat and L. Vandendorpe, "On the Number of RF Chains and Phase Shifters, and Scheduling Design With Hybrid Analog–Digital Beamforming," in *IEEE Transactions on Wireless Communications*, vol. 15, no. 5, pp. 3311-3326, May 2016.

[18] Y. Lin, "On the Quantization of Phase Shifters for Hybrid Precoding Systems," in *IEEE Transactions on Signal Processing*, vol. 65, no. 9, pp. 2237-2246, 1 May1, 2017.

[19] X. Yu, J. Zhang and K. B. Letaief, "Doubling Phase Shifters for Efficient Hybrid Precoder Design in Millimeter-Wave Communication Systems," in *Journal of Communications and Information Networks*, vol. 4, no. 2, pp. 51-67, June 2019.